Ice-Assisted Preparation of Silica-Supported Vanadium Oxide Particles

S. Kaya, Y.-N. Sun, J. Weissenrieder, D. Stacchiola, S. Shaikhutdinov,* and H.-J. Freund

Fritz-Haber-Institut der Max-Planck-Gesellschaft, Faradayweg 4-6, 14195 Berlin

Received: December 21, 2006; In Final Form: February 2, 2007

Vanadium oxide particles were prepared by physical vapor deposition of vanadium in oxygen ambient onto ice-precovered well-ordered silica thin films. Morphology, electronic structure, and vibrational properties of the vanadia deposits were studied by scanning tunneling microscopy, X-ray photoelectron spectroscopy, temperature-programmed desorption, and infrared reflection absorption spectroscopy. The results show that the ice behaves as an oxidative agent, that favors vanadium oxidation up to V^{4+}, and as a buffer layer that precludes strong interaction of the V adatoms with the silica film. At room temperature, upon desorption of the unreacted water, nanosized particles of vanadia hydroxide-like gel, containing V−OH and, to a lesser extent, vanadyl (V=O) species, are formed. Vacuum annealing at 550 K leads to the total dehydration and partial reduction of the particles to V_2O_3, which expose the V-terminated surface. Subsequent reoxidation in 10^{-6} mbar of O_2 irreversibly transforms the surface to the V=O terminated, that is, the same as for the reactive deposition onto the clean silica surface. The results suggest that the structure of silica-supported vanadia catalysts is determined by a calcination step and should be considered under low oxygen pressure conditions as vanadium sesquioxide nanoparticles with the V=O terminated surface.

1. Introduction

During recent decades, a vast amount of studies were reported in the literature on the structural characterization of vanadium oxides, which, when supported at submonolayer coverage onto other oxides, were found to be effective catalysts for many industrially important reactions such as selective oxidation of methanol to formaldehyde,[1] oxidative dehydrogenation of propane to propene,[2] and selective catalytic reduction of NO_x.[3] By employing different experimental and theoretical approaches, these studies have shown that there are several factors which contribute to the functionality of the vanadia-based catalysts such as vanadia loading, nature of the oxide support, degree of hydration, etc.

Among others, Raman spectroscopy seems to be the most frequently used technique for characterization of the surface structure of the vanadia-based catalysts.[2,4] Although the nature of many absorption bands in the spectra is generally understood, such as of vanadyl (V=O) species, there are continuing debates in the literature on the precise determination of the fraction of isolated versus polymeric vanadate species and also on the nature of the vanadia/support interface sites.[5,6] It is well documented that, for the powdered catalysts, the frequency of the V=O stretching varies in the range between 1040 and 1010 cm^{-1} depending on the support and vanadia loading.[5−7] A band at 995 cm^{-1} has also been reported for samples containing V_2O_5 crystallites.[8] In addition, a broad band at around 920 cm^{-1} seen in the Raman spectra at high vanadia loadings on alumina and titania supports has been attributed to formation of polymeric (V−O−V) species.[7] However, using model systems, Magg et al.[9] have recently revised the assignment of this low-frequency band and suggested that it must be attributed to the vibrations involving interface V−O−Al bonds. Very recently, on the basis of X-ray absorption results and further theoretical studies, Keller

et al. have suggested the "umbrella" model[10] for the monomeric VO_4 species, describing them as $O_{support}$−V=O(O_2) species with only one V−O-support bond, in contrast to the commonly accepted pyramidal model with a V=O bond and three V−O-support bonds. In this model, the Raman band at 915 cm^{-1} has been assigned to an O−O stretching vibration.[11]

To understand structure−reactivity relationships in catalysis by oxides on a fundamental level, planar model systems with reduced complexity have been invoked.[12,13] When applied to the vanadia-based systems, these models can be formally divided in two groups: (1) thin vanadium oxide films and (2) vanadia supported on well-ordered oxide films. The atomically flat vanadium oxide films have been grown on a variety of single-crystal substrates like Cu(100),[14] Au(111),[15] W(110),[15] Cu_3Au-(100),[16] and Pd(111).[17] It was shown that the vanadia films exhibit V_2O_3(0001) structure, however, the surface exposes V=O groups. When deposited on alumina and silica films at submonolayer coverage, vanadia always formed three-dimensional nanoparticles, which exhibited electronic structure and vibrational properties very similar to those of the V_2O_3 films.[9,18,19]

As a next step in our modeling of the vanadia-based catalysts, we have in this work examined the effect of water on the growth and structure of vanadia supported on the thin silica films, which could, to a certain extent, mimic "wet" preparation of the supported catalysts. In a recent study, we showed that water exposed to the silica films formed so-called amorphous solid water (ASW) films at $T < 120$ K which transforms into the crystalline ice (CI) above 130 K and sublimates in vacuum above 160 K.[20] Since the silica film is essentially inert toward water,[20,21] the vanadium deposition was performed on an ice film formed on the silica substrate at low temperatures. Ice overlayers were previously used by Yan et al.[22] for the synthesis of silver nanoparticles. Liang and Perry[23] adopted the same

approach to Cu. Song et al.[24] showed the influence of the ice film on stability of TiO_2 crystallites grown onto a Au(111) substrate.

The paper is organized as follows. First, we summarize the key observations for the morphology, electronic structure, and vibrational properties of the vanadia clusters supported on the silica films in light of recent determination of the atomic structure of these films. Then, we present in details the results of the structural characterization of the vanadia deposited on the water-precovered films using scanning tunneling microscopy (STM), X-ray photoelectron spectroscopy (XPS), temperature-programmed desorption (TPD), and infrared reflection absorption spectroscopy (IRAS). Finally, we discuss the role of water in the preparation of vanadia/silica model catalysts and conclude with a summary.

2. Experimental Section

The experiments were carried out in two ultrahigh vacuum (UHV) chambers (base pressure $<2 \times 10^{-10}$ mbar). One chamber was equipped with low-energy electron diffraction (LEED, Omicron), XPS (Scienta SES-200 analyzer), IRAS (Bruker i66/vs), STM (Omicron), and standard facilities for sample cleaning.[25] The Mo(112) crystal ($7 \times 5 \times 1.5$ mm^3, Matek) was clamped to a Mo sample holder having a 6-mm hole for electron bombardment heating from the backside of the crystal.

TPD experiments were performed in another UHV chamber equipped with a quadrupole mass spectrometer (QMS, Fisions) and four-grid optics for the LEED/Auger electron spectroscopy (AES) studies. The Mo crystal was spot-welded to two parallel W wires used for resistive heating and cooling with a liquid nitrogen reservoir. In both chambers, the temperature was measured by type C (W−Re) thermocouple spot-welded to the edge of the crystal.

The Mo(112) surface was cleaned by cycles of oxidation in 1×10^{-6} mbar O_2 at 800 K and flash annealing to 2300 K in vacuum. The surface cleanliness was checked by XPS or AES. In the TPD chamber, heating to the very high temperatures was achieved by an external W filament placed close to the backside of the crystal.

Metallic Si and V (both 99.99%, Goodfellow) were deposited from rods of 2 mm in diameter using electron beam assisted evaporators (Focus EFM3). During evaporation, the substrates were biased to the same potential as the evaporating rods to prevent metal ions accelerating toward the sample.

Preparation and atomic structure of well-ordered thin silica films are described elsewhere.[26] Vanadium was deposited onto the pristine or water-precovered silica films to the amounts presented in the paper in monolayers (ML, 1 ML = 5×10^{14} atoms/cm^2) with a rate of ca. 0.2 ML/min as calibrated by a quartz crystal microbalance. In all experiments, vanadium was deposited in 2×10^{-7} mbar O_2 at 100 K if not specified. Oxygen (Linde Gas, 99.9995%) was dosed by backfilling the chamber using a high-precision leak valve. Doubly distilled water was cleaned by several freeze−pump cycles and was checked by QMS prior to use. The silica substrate was exposed to water vapor at 100 K (ca. 5×10^{15} molecule/cm^2), which is equivalent to grow approximately five bilayers of ice (BLE) as calibrated by a water monolayer film on Pt(111). Water and CO were exposed to the samples using a directional gas doser.

The binding energies (BE) in the XP-spectra were calibrated relative to the Fermi edge of the Mo substrate. XPS measurements were performed using an Al Kα ($h\nu = 1486.6$ eV) source for the O1s and V2p levels and a Mg Kα ($h\nu = 1253.6$ eV)

source for the Si2p level. Spectra deconvolution for both V2p and O1s levels was performed using a combination of Gaussian and Lorenzian profiles with the Doniach−Sunjić[27] line shape. Best fit was obtained with Shirley background subtraction.[28]

IRAS experiments were carried out with p-polarized light at 84° grazing angle of incidence. TPD experiments were done by placing the sample <1 mm away from the aperture of the gold-plated shield of the QMS to diminish the signals coming from the heating wires. Sample temperature and heating rate (3 K/s) were precisely controlled by a feedback system (Schlichting Phys. Instrum.).

All STM images were recorded at room temperature in a constant current mode. The bias voltages are referred to the sample.

3. Results

3.1. Vanadia Supported on a Clean Silica Film. The atomic structure of the crystalline silica film has been previously studied by our group in details.[20,26,29,33] Basically, the silica film consists of a two-dimensional network of corner-sharing [SiO$_4$] tetrahedra, with one oxygen of each tetrahedra bonding to the Mo substrate atoms.

Figure 1 summarizes the key observations for vanadia supported on the clean silica films. Vanadium deposition in 2×10^{-7} mbar of O_2 at 300 K results in three-dimensional nanoparticles, which are randomly distributed on the surface (Figure 1a, b). (At oxygen pressures used, vanadium oxidation and clustering occurs on the surface and not in the gas phase.) At low coverage, the morphology of the silica substrate, forming wide terraces separated by monatomic steps of ca. 0.12 nm in height, can be also recognized. Comparing these STM images with those observed for Au, where particles are mostly found on the step edges (not shown here), one can conclude that the V adatoms quite strongly interact with the silica film and therefore exhibit a low diffusivity. As a result, the particle density increases remarkably while the mean particle size that ranges between 0.4 and 1.2 nm stays nearly the same at increasing coverage up to 1 ML.

The O1s and V2p regions in the XP-spectra are shown in Figure 1c. Since the V2p core level shows two spin−orbit components, we will hereafter, for simplicity, only refer to the V2p$_{3/2}$ component. The bottom curve in this figure shows the spectrum for the silica film, which exhibits two O1s lines centered at 532.5 and 531.2 eV. These states have previously been assigned to the O atoms in the topmost layer, formed by sharing three oxygen atoms of [SiO$_4$] tetrahedra, and to the O atoms linking Si and the Mo substrate atoms, respectively[26,29] (e.g., see inset in Figure 2a). At increasing V coverage, the O1s signal grows in intensity until only a symmetric peak at 530.4 eV is observed, which is typical for the BEs of oxygen in many transition-metal oxides.[30]

Regarding the valence state of vanadium, a broad signal centered at 513 eV is observed at low and mid coverages which is characteristic for the metallic state.[31] In addition, initially fully oxidized Si^{4+} atoms were found partially reduced after reactive vanadia deposition (not shown here). This again indicates a strong interaction of the V atoms with the silica film proposed above on the basis of STM images. It seems plausible that the V adatoms migrate into the hexagonal rings, present in the structure of the silica film, as theoretically predicted by Giordano et. al for Pd.[32] The fact that such a strong interaction was not clearly observed in the previous studies[9] may be related to that

Silica-Supported Vanadium Oxide Particles
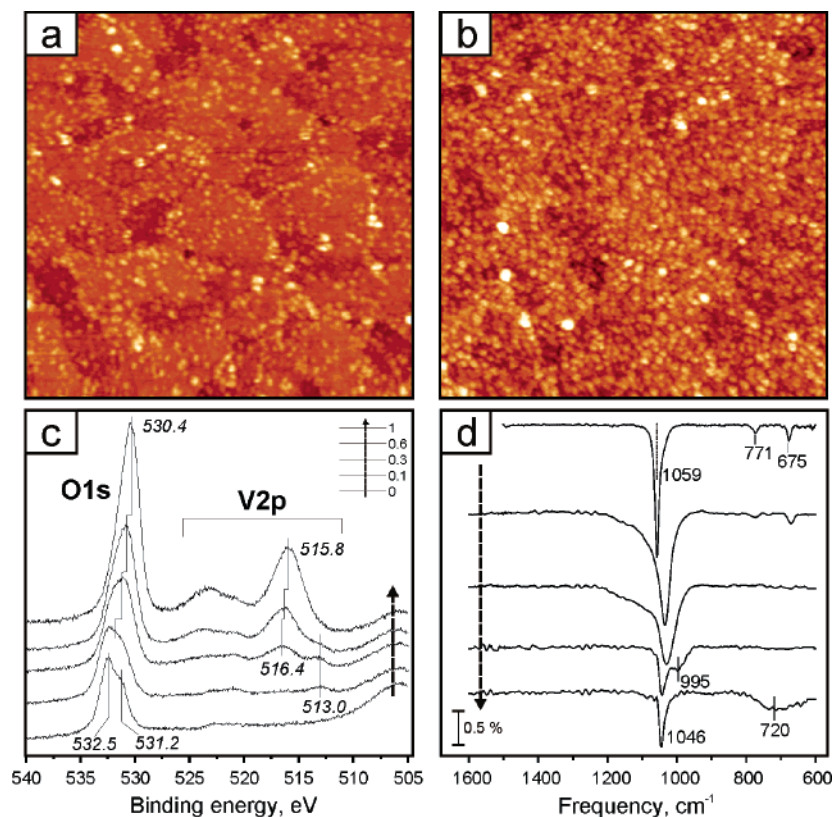
J. Phys. Chem. C, Vol. 111, No. 14, 2007 **5339**

Figure 1. STM images (100×100 nm^2) of 0.12 ML (a) and 0.4 ML (b) vanadium oxide particles formed by deposition on the silica film in 2×10^{-7} mbar O$_2$ at 300 K. (Tunneling parameters: $V_S = 3$ V, $I = 0.2$ nA). The XP-spectra (c) and IRA-spectra (d) are shown as a function of V coverage, indicated in c. All measurements were performed at 300 K.

those silica films were less ordered and "O-rich" in nature,[33] which may alter the interaction.

At increasing coverage, a high BE peak emerges and dominates the spectra. This peak slightly shifts from 516.4 eV at 0.3 ML to 515.6 eV at 1 ML probably because of vanishing of the well-known final state effect, leading to higher BE values for the smallest particles. The last spectrum is in fact very similar to that observed on well-ordered V$_2$O$_3$ films,[15,34] thus suggesting that the oxide particles formed on the silica films under these conditions are of V$_2$O$_3$ in nature.

Finally, Figure 1d shows IRAS spectra for the vanadia/silica surface as a function of V coverage. On the clean silica film, a very intense peak at 1059 cm^{-1} corresponds to the Si−O−Mo asymmetric stretching, and the two weak absorption bands at 771 cm^{-1} and 675 cm^{-1} are assigned to combination of Si−O−Si stretching and bending modes, respectively.[29] Vanadia deposition leads to a broadening and shift to lower frequencies of the main silica phonon with increasing coverage. Concomitantly, the band at 1046 cm^{-1} grows up, which is assigned to the stretching vibration of V=O species. A broad signal centered at 720 cm^{-1} that emerges at the highest coverage studied can be assigned to the V−O−V stretching vibrations in the bulk vanadia.[35]

Therefore, a combined STM, XPS, and IRAS study shows that vanadium deposited in oxygen ambient strongly interacts with the ultrathin silica film and forms V$_2$O$_3$-like nanoparticles exposing V=O surface species.

3.2. Vanadium Deposition on an Ice-Precovered Silica Film. Water adsorbed onto the silica film at 100 K forms an amorphous solid water (ASW) film, which transforms into crystalline ice (CI) on heating above 130 K.[20] On further heating, the ice sublimates showing a zero-order desorption kinetics, with a desorption peak in TPD spectra gradually shifting to the higher

temperatures with increasing initial coverage ($\sim$160 K for 5 BLE). This ice layer may form an ordered structure with respect to the silica substrate as previously shown.[20] No water dissociation has been observed on these silica films.[20,21] The XPS and IRAS inspection of the films after water adsorption− desorption cycles did not reveal any structural changes, for instance, formation of an O-rich film, which would otherwise result in well-resolved spectral changes.[33]

3.2.1. Morphology. Figure 2a−c shows the room-temperature STM images of vanadium deposited onto the ASW film at 100 K in 2×10^{-7} mbar O$_2$ as a function of V coverage. At very low coverage (<0.1 ML), the majority of the particles are located on the steps. In addition, high-resolution images often showed atomic-size features (see inset in a), which could be assigned to "monomeric" species. Registry analysis revealed that these species likely sit above the outmost Si−O−Si bonds of the [SiO$_4$] network as schematically shown in the model.

Step decoration by the particles at increasing coverage is clearly seen in Figure 2b. The apparent height and lateral size distributions of the particles are in the range of 0.4−1.5 nm and 1.5−4 nm, respectively. Most of the particles are ill-defined and not well-shaped, however, some very small particles found on the terraces were elongated in the Mo[$\bar{1}$10] direction, which coincides with one of the principal directions of silica network, as shown in the inset in Figure 2b.

At further increasing coverage, the particles grow in size and tend to aggregate. In addition to the particles accumulated at step edges, the aggregates on the terraces show chains of particles, which are difficult to discriminate because of the presence of the strongly bonded water shell at 300 K (see TPD results below) that smoothes the surface of the connected particles. Isolated small particles form areas of a high-packing
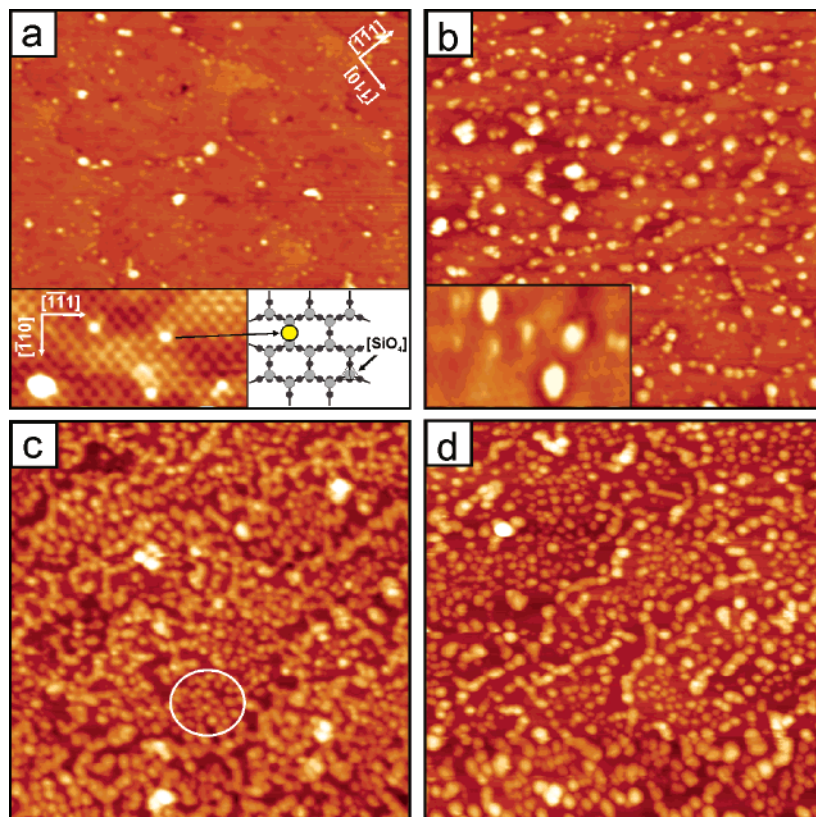
Figure 2. Room-temperature STM images (100×100 nm^2) of V deposited at 100 K in 2×10^{-7} mbar O$_2$ onto $\sim$5 BLE water film grown onto a silica substrate at 100 K. The V coverage is 0.035 ML (a), 0.15 ML (b), and 0.5 ML (c). Image (d) shows the same sample as in (c) after flash annealing to 600 K. Tunneling parameters (bias/current) are (a, b) 4.0 V/0.2 nA, (c, d) 3.0 V/0.2 nA. The inset in (a) (size 10×4 nm^2, tunneling parameters 1.2 V/0.3 nA) shows the atomic size features, which can be assigned to monomeric V=O species sitting above the outmost Si−O−Si bonds of the [SiO$_4$] network as schematically shown in the model. The inset in (b) (12×8 nm^2; 1.0 V/0.18 nA) zooms in the portion of the image (a), where the articles are found elongated along the Mo[$\bar{1}$10] direction.

density, which are separated or surrounded by the larger aggregates as outlined by the circle in Figure 2c.

The particle density remains practically the same after subsequent heating to 600 K, therefore indicating a good resistance of the particles toward sintering. However, the particles became apparently smaller (as shown in Figure 2d) because of removal of the water shell and vanadia recrystallization.

3.2.2. Temperature-Programmed Desorption (TPD). As mentioned above, water desorbs from the silica film in a single desorption peak following zero-order kinetics.[20] Since in the excess of water (typically 5 BLE) this desorption peak masks desorption from the vanadia deposits, Figure 3a shows desorption spectra for the samples preheated to 300 K to desorb the weakly bonded water from the silica. Only hydrogen (2 amu) and water (18 amu) are found desorbing from the surface on heating to 600 K. The results clearly indicate that water strongly interacts with the vanadia particles.

Figure 3b shows TPD spectra of CO used as a probe molecule for the cationic V sites.[36] The sample was first heated to 225 K (to remove the unreacted water) and then was subjected to CO TPD runs (cycles of CO adsorption−desorption) with stepwise increasing the final temperature (250, 300 K, etc). For each TPD run, the same amount of CO (1 L) was adsorbed at 100 K to quantify the fraction of the surface sites accessible to CO upon partial dehydration. Small amounts of CO may adsorb on the defect sites of the silica film which in addition to the parasitic signal from the heating wires result in a broad desorption feature at 120−200 K.

A well-resolved CO desorption peak at $\sim$205 K, gradually increasing in intensity, is observed on the samples heated to

225−300 K. Dehydration above 300 K makes another adsorption site accessible for CO from which it desorbs at $\sim$160 K. The desorption signals overlap after dehydration at 500 K. No further changes in CO TPD spectra are observed after annealing to 600 K, that is, in line with the complete dehydration of the sample as can be deduced from Figure 3a. Oxidation of the fully dehydrated sample in 2×10^{-7} mbar of O$_2$ at 600 K strongly and irreversibly reduces the CO adsorption capacity, which can be explained by the formation of an oxygen-terminated surface which is inert toward CO. The latter spectrum is very similar to that observed on the pristine silica film.

3.2.3. X-ray Photoelectron Spectroscopy (XPS). Comparison of electronic structures of vanadium oxides by XPS, in particular at low and high temperatures, is not straightforward since several vanadium oxide phases (like VO$_2$, V$_6$O$_{13}$, and V$_2$O$_3$) exhibit metal-to-insulator phase transition[37,38] that may in turn depend on the film thickness,[39] doping,[40] and structural relationships to the substrate.[41] In addition, the V^{4+} and V^{3+} states are known to show core levels broader than that of the V^{5+} state because of Coulombic interaction of the core hole with the 3d electrons.

Figure 4a shows XP-spectra of the $\sim$2 BLE water/silica film exposed to increasing amounts of vanadium. (We have reduced water coverage to minimize the charging effects.) At low coverage ($<$0.2 ML), the V2p$_{3/2}$ signal is broad and centered at around 515 eV, which is typical for the V^{3+} state.[31,42,43] Vanadium deposition on the water film without oxygen in the ambient also resulted in the V^{3+} state, with an asymmetric line shape and a slightly (ca. 0.3 eV) lower BE value, though.

In the O1s region, the spectrum is dominated by the broad signal of water at $\sim$533.5 eV. As more water molecules interact with the V atoms at increasing coverage, the signal shifts to

Silica-Supported Vanadium Oxide Particles

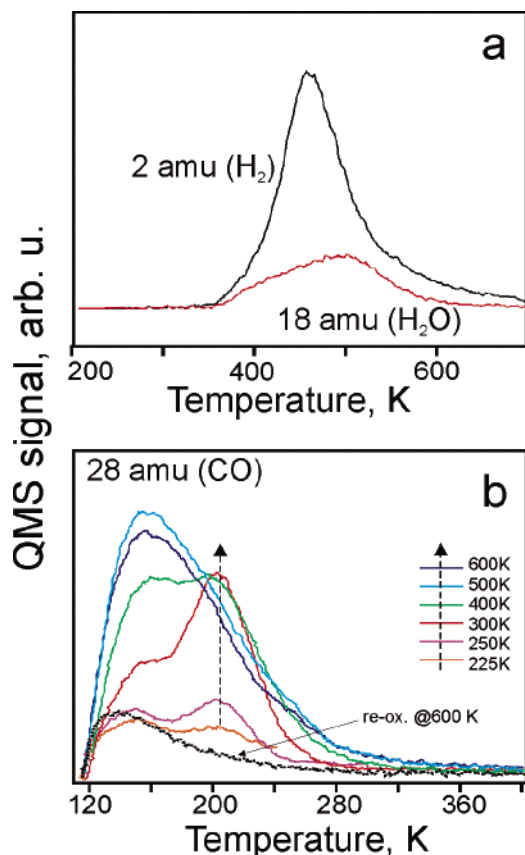*J. Phys. Chem. C, Vol. 111, No. 14, 2007* **5341**

Figure 3. (a) The 2 (H_2) and 18 amu (H_2O) desorption traces from the 0.8 ML V deposited onto ~5 BLE water/silica film at 100 K and then heated in vacuum to 300 K. (b) TPD spectra of 1 L CO adsorbed at 100 K on the similarly prepared sample first preheated to 225 K. The CO TPD measurements were repeated while stepwise increasing the end temperature as indicated. CO adsorption capacity increases on dehydration and is strongly reduced after reoxidation of the dehydrated sample at 600 K. Heating rate is 3 K/s in all spectra.

lower BE, ultimately leading to the broad signal at 532.6 eV, which is about ~2 eV higher than observed for the V_2O_3 particles and films.[19,44] Tentatively, this high-binding energy has been assigned to hydroxyl species, which are masked by the molecular water present at 100 K. Indeed, warming to 300 K shifts the signal to ~530.5 eV, that is, typical for vanadium oxides.

Figure 4b shows that at 100 K the $V2p_{3/2}$ signal consists of at least three states, denoted as V1, V2, and V3 (see the deconvolution details in Experimental Section). Since the V3 state emerges on deposition first (see Figure 4a), it can be associated with the initial interaction of the first soft-landing V atoms with the dangling hydroxyl groups on the ice surface and the formation of a state in a comparably low formal oxidation state. The fact that the whole spectrum apparently shifts by ~0.3 eV to lower BE upon heating to 300 K may be explained by size and charging effects of the vanadia species formed at 100 K and their agglomeration on heating. The V3 component almost entirely disappears upon heating to 300 K, while the most prominent V2 state at 516.5 eV, which is within the range reported for V^{4+},[31,42,43] gains intensity. The V2 state must be attributed to the major structure of the particles observed by STM (Figure 2).

Annealing to 600 K fully dehydrates the particles, as shown above by TPD, and shifts the V2 state into the V^{3+} range (515.8 eV). The relative intensity and position of the V1 and V3 components changes only slightly. Subsequent oxidation at
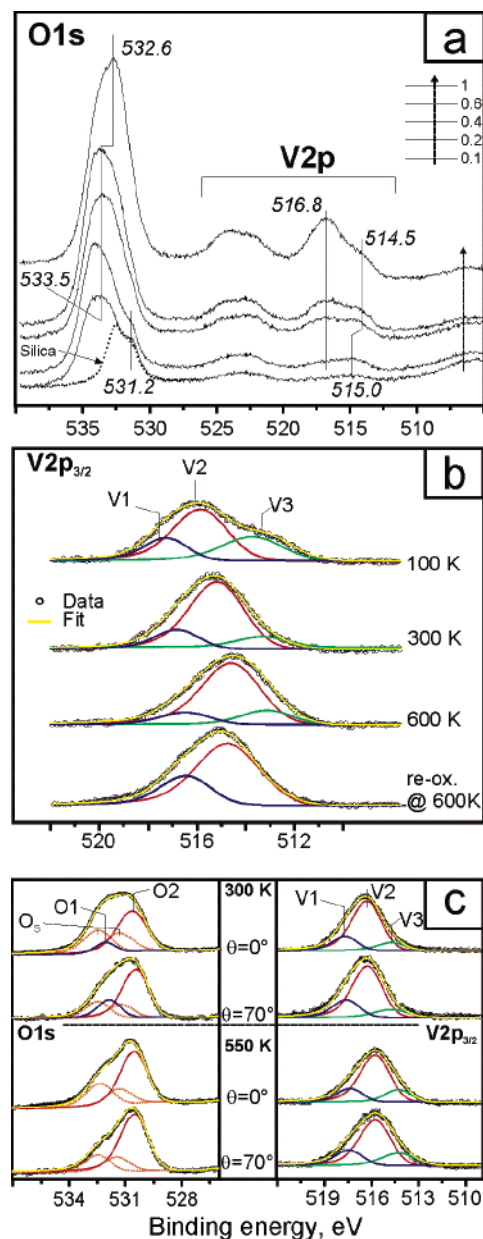

Figure 4. (a) O1s and V2p photoemission spectra of V deposited at 100 K on the ~2 BLE water/silica film as a function of V coverage as indicated. (b) The deconvolution analysis of the 1 ML V sample measured at 100 K, after flash to 300 and 600 K, and after reoxidation at 600 K. (c) The O1s (left panel) and $V2p_{3/2}$ (right panel) XP-spectra of the 1 ML V sample taken at normal (0°) and grazing (70°) emission angles and their deconvolution analysis.

600 K in 2×10^{-7} mbar of O_2 increases the population of the V1 state and totally suppresses the V3 states. This is similar to what previously has been observed by XPS for the vanadyl-terminated V_2O_3(0001) surface[34] and, therefore, the V1 component can be attributed to V=O species.

The O1s signal at 300 K (left panel in Figure 4c) revealed two oxygen states, at least, (O1 and O2) beyond those of silica (O$_S$). This implies a structure comprising V−O−V and V−OH bonds within the nanoparticles observed by STM in Figure 2. The O2 component at 530.4 eV is typical for different 3d metal oxides and has been observed on vanadia particles prepared without water (see Figure 1c). Therefore, it can be assigned to V−O−V species. Meanwhile, the O1 state at 531.7 eV, disappearing at 550 K, is characteristic for hydroxyl groups adsorbed on oxide surfaces as reported for V_2O_3,[45] TiO_2,[46] and

Cr$_2$O$_3$.[47] Therefore, these results favor the model of vanadium oxide particles exposing OH species on the surface.

In attempts to further understand the structure of the particles, we have measured XP-spectra at two different electron emission angles, 0° and 70° with respect to the normal (see Figure 4), which could in principle discriminate surface versus bulk species in a multicomponent system, although the angular sensitivity in experiments using a conventional X-ray source is rather limited because of the relatively high kinetic energy of the photoelectrons (~950 eV).

Nevertheless, it is found that the relative intensity of the V1 component as compared to the main V2 signal is always higher at grazing than at normal emission for both hydrated (at 300 K) and dehydrated (at 550 K) samples. This is consistent with the above assignment of the V1 state to V=O species whose intensity grows remarkably by oxidation of the dehydrated samples (see Figure 4b).

The situation with the O1s states is complicated by the presence of oxygen states in the silica substrate, whose contribution is also angle-dependent. Therefore, we first look at the sample annealed to 550 K, where water and hydroxyls are no more present, and therefore only the O2 and O$_S$ components are involved. This allowed us to find an attenuation factor for the silica substrate measured at 70° versus 0°, which was then used for the hydrated sample at 300 K. Using this approach, we found that the relative intensity of the O1 component with respect to O2 is higher at grazing emission, thus indicating that these species are more surface related and therefore can be assigned the surface hydroxyl groups on the vanadium oxide particles.

3.2.4. Infrared Reflection Absorption Spectroscopy (IRAS). Our previous IRAS study showed that the ASW overlayer shifted the main silica phonon at 1059 cm^{-1} (see Figure 1d) by 8–10 cm^{-1} to higher frequencies, at most.[20] However, the ordered CI layer shifted it to a higher extent (~25 cm^{-1}) and exhibited an isotopic effect (H$_2$O vs D$_2$O). These blue shifts have been tentatively assigned to polarization of the Si−O− Mo bond by the adsorbed water molecules.

Curves 1–4 in Figure 5a show IRA-spectra at 100 K as a function of V coverage. It is clear that the vanadia deposits cause a blue shift by far larger than the ASW layer itself (1110 vs 1068 cm^{-1}), and this shift is almost independent of the V coverage. In contrast, vanadium deposition only slightly (by ca. 8–11 cm^{-1}) affects the stretching and stretching−bending vibration modes of the Si−O−Si bond at 760−680 cm^{-1}.

Figure 5b shows the OH-stretching region of the water/silica film before and after vanadium deposition at 100 K (curves 1 and 2, respectively). A broad band between 3600 and 3000 cm^{-1} and small peak at 3696 cm^{-1} are typical for the stretching mode of H-bonded and "isolated" dangling OH groups, respectively.[48] Vanadium deposition strongly reduces the intensity of the bands assigned to the free water, and a prominent shoulder at 3625 cm^{-1} appeared, which is more clearly seen after water desorption at 300 K (curve 3 in Figure 5b). This band is in the range of the O−H stretching vibrations observed in hydrated vanadium oxides[49] as well as for hydroxyl species on the vanadia surfaces.[44]

After partial dehydration by heating to 300 K, the silica phonon shifts almost back to the initial value of the clean silica, and a band centered around 1035 cm^{-1} appears as a shoulder (curve 5 in Figure 5a). Only the latter band remains upon further annealing to 600 K, which is in fact very similar to that observed on the vanadia deposited on the clean silica film to the same coverage (see Figure 1d). Postoxidation at 300 K broadens the
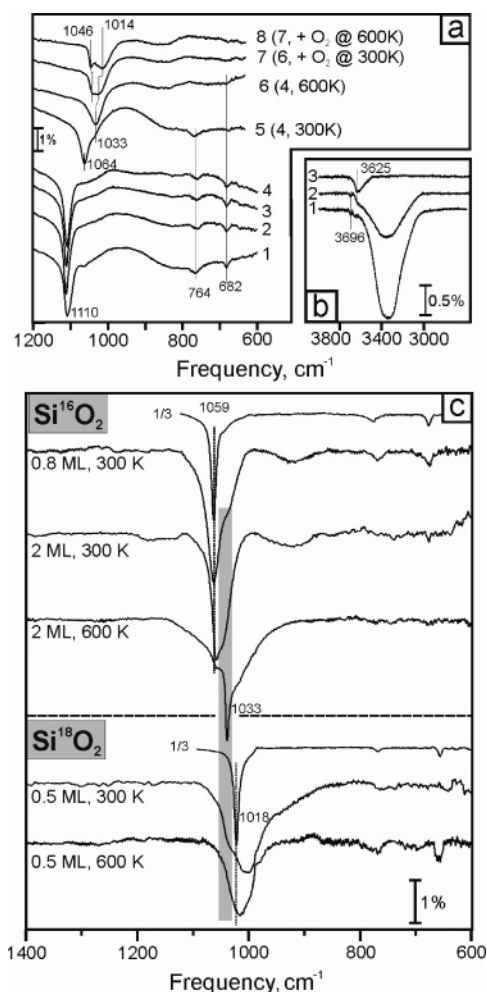

Figure 5. (a) Silica phonon region of the IRA-spectra measured at 100 K after deposition of the 0.1, 0.2, 0.4, and 0.6 ML on the ~5 BLE water/silica film (curves 1−4). Curves 5−8 show the spectra for the same 0.6 ML sample as for curve 4 heated to 300 and 600 K in vacuum and then oxidized in 1 × 10^{-7} mbar O$_2$ at 300 and 600 K, respectively. (b) IRAS spectra of the OH stretch region of the pure ~5 BLE water/silica film at 100 K (curve 1), followed by deposition of 0.4 ML V in 2 × 10^{-7} of O$_2$ at 100 K (2) and heating the same sample to 300 K (3). (c) IRAS spectra on the clean silica (×$^1/_3$) and V/water/silica samples with the silica film prepared with ^{16}O (upper panel) and with ^{18}O (bottom panel). The V coverage and temperatures are indicated. In both cases, normal water (H$_2$^{16}O) was used for the growth of the ice film.

spectrum from the high-frequency side and leads to a well-resolved peak at 1046 cm^{-1} upon oxidation at 600 K (curves 6 and 7, respectively) because of the formation of V=O species.

The band at 1035 cm^{-1} observed after partial dehydration at 300 K deserves a closer look. It is known that the stretching frequency of V=O surface species depends on the degree of hydration of vanadium oxide.[50−52] Therefore, this peak could, in principle, be assigned to some amounts of the V=O groups present among the moiety of the V−OH species. However, the presence of the silica phonon vibrations in the same frequency region makes their discrimination difficult. To clarify this issue, we have performed experiments with silica films prepared with ^{18}O$_2$, for which the main silica phonon is shifted to 1018 cm^{-1} as shown in Figure 5c. Similar to the spectrum (5) in Figure 5a, the spectra for partially dehydrated samples of vanadia on the Si^{16}O$_2$ film at 300 K exhibit a prominent shoulder on the low frequency side of the silica phonon. Meanwhile, the similar experiments with the Si^{18}O$_2$ film showed the shoulder on the high frequency side. However, both these signals fall

Silica-Supported Vanadium Oxide Particles

J. Phys. Chem. C, Vol. 111, No. 14, 2007 **5343**

into the region $1025-1045$ cm^{-1} typical for V=^{16}O species, which are formed from normal water, H$_2$^{16}O. This finding suggests that vanadia particles at 300 K can, in principle, contain vanadyl species in addition to hydroxyls. Interestingly, the 2 ML V sample fully dehydrated at 600 K showed a very sharp peak at 1033 cm^{-1} that indicates a long-range surface ordering.

4. Discussion

We have previously shown that water adsorbed onto the silica film at ~100 K forms an ASW or "amorphous ice" film, which transforms into crystalline ice upon heating to ~130 K and sublimates above 160 K.[20] When exposed at 100 K in the amounts equivalent to ~5 BLE of ice used in our experiments, the silica film seems to be uniformly covered by water clusters and their aggregates, although no STM data are available to date.

The V atoms, soft landing on the ice film, strongly react with the water surface molecules and become oxidized to V^{3+}−V^{4+} states as shown by XPS (see Figure 4a). Indeed, vanadium deposition on the water/silica substrate without oxygen in the ambient also resulted in a V^{3+} state. In the presence of water, the V2p binding energies are significantly higher, at a given V coverage. Therefore, we conclude that water serves as an oxidation agent and facilitates vanadium oxidation. In addition, the water film behaves as a buffer layer precluding strong interaction of the V atoms with the silica film, which is observed on the pristine substrate (see Figure 1c).

According to the IRAS data, vanadium deposition reduces the intensity of the ice-related OH bands and gives rise to a signal at 3625 cm^{-1}, which is characteristic for chemisorbed OH species on transition-metal oxide surfaces. (The silanol (Si−OH) groups would manifest itself at around 3750 cm^{-1} [53,54] and therefore are not formed under these conditions.) It appears that it is water dissociation by vanadium that results in the strong blue shift of the silica phonon (see Figure 5). This hypothesis is further supported by the fact that similar effect has been observed after prolonged exposure of the pure ASW film to X-rays or low-energy electrons, which may cause dissociation and ordering in water overlayers.[55,56]

The diffusivity of proposed V(OH)$_x$ species at 100 K is expected to be low, however, they may aggregate at high coverage. However, two different V species are observed in XP-spectra at increasing V coverage (see Figure 4a), which may be indicative for different reaction sites for V with the ASW particles, for example, on the surface and in the bulk, but this issue needs further studies.

Nonetheless, heating to the room temperature results in the formation of small particles and agglomerates as revealed by STM in Figure 2. The agglomeration seems to reflect a different growth mode as compared to the deposition on the clean silica. The growth is governed not only by the interaction of the V atoms with a substrate but also by the subsequent water crystallization−sublimation processes, which are not well controlled as it may depend on the ice thickness, heating rate, etc. For example, Yan et al.[22] suggested a model where silver particles were confined in droplets of a metastable phase of liquid water, as previously proposed by Smith and Kay.[57] In a similar way, Song et al.[24] rationalized growth of TiO$_2$ nano-particles on the water/Au(111) surface. However, recent studies[58] highlight the importance of the ice film cracking during the crystallization, which may ultimately influence the morphology.

TPD analysis of the samples preheated to 300 K showed water desorbing up to 500 K (Figure 3a) most likely through recombination of OH and H surface species formed upon water dissociation by vanadium at 100 K. Simultaneous evolution of H$_2$ as a result of recombination of H species in addition to the fact that the H$_2$ desorption reaches a maximum at temperatures by ~50 K lower than of H$_2$O indicates that water can also be desorbing through recombination of more strongly bound hydroxyl species, as it has been previously observed on the V$_2$O$_3$,[44,45] TiO$_2$,[59] and Fe$_3$O$_4$[60] surfaces.

At the room temperature, the system is basically represented by vanadia particles in average oxidation state around +3.5, which contain OH species mostly on the surface as shown by IRAS and angular-resolved XPS. However, the presence of V−OH species also in the bulk cannot be ruled out from these experiments. The results of isotopic IRAS experiments suggest that the surface may in addition expose V=O species, in particular at high V coverage (Figure 5c). Since stretching frequency of V=O species depends on the degree of dehydration, its observation can be obscured by the silica phonon. It seems plausible that the particles formed under these conditions exhibit a rather complex stoichiometry similar to vanadium hydroxide gels.

Annealing to 500−600 K strongly increases the CO adsorption capacity (Figure 3b), which is consistent with removing the OH species bonded to V and hence increasing the amount of the cationic sites accessible to CO. Therefore, in contrast to the deposition onto the clean silica film, ice-assisted preparation allows formation of V-terminated particles upon dehydration treatment. These particles are stable toward sintering up at 600 K and only become apparently smaller because of dehydration (see Figure 2c, d).

Reoxidation of the dehydrated samples leads to the formation of a vanadyl-terminated surface as evidenced by XPS and IRAS. As a result, the surface is essentially inert toward CO and is very stable toward reduction, that is, similar to the V=O terminated V$_2$O$_3$ particles and films.[61,62]

5. Summary

We used a thin ice film as a reactive layer in the preparation of silica-supported vanadium oxide model catalysts. The results suggest that the ice behaves as an oxidative agent that favors vanadium oxidation up to V^{4+}. Nucleation and growth mode of vanadia on the ice-precovered silica films is found to be different as compared to that on the clean silica surface. Although formation of small nanoparticles has been observed in both cases, water precludes the strong interaction of the metallic V adatoms with the thin oxide film.

The combined STM, TPD, XPS, and IRAS results suggest that the vanadium atoms, soft landing on the ASW surface, dissociate water molecules and form V(OH)$_x$ species and their aggregates in average oxidation state +3.5. Heating to the room temperature results in desorption of the unreacted water and agglomeration of the vanadia species during a complex water crystallization−sublimation process, ultimately forming small particles of vanadium hydroxide gel, which expose V−OH and, to a lesser extent, V=O surface species.

Total dehydration of the samples at elevated temperatures (above 500 K) leads to the formation of V-terminated V$_2$O$_3$ particles. The phase transition, accompanying water removal, proceeds without significant sintering of the nanoparticles. Subsequent oxidation by oxygen at 300−600 K leads to the V=O terminated surface.

The results show that water does not lead to vanadia wetting the oxide substrate (at least, at submonolayer coverage), as envisaged in supported "monolayer-type" vanadia catalysts. Therefore, the results further support a conclusion that the

structure of the silica-supported vanadia catalysts under low oxygen pressure conditions used in the model studies should be considered as vanadium sesquioxide nanoparticles with a surface exposing vanadyl groups.

References and Notes

(1) Deo, G.; Wachs, I. E. *J. Catal.* **1994**, *146*, 323.

(2) Khodakov, A.; Olthof, B.; Bell, A. T.; Iglesia, E. *J. Catal.* **1999**, *181*, 205.

(3) Bond, G. C.; Tahir, S. F. *Appl. Catal.* **1991**, *71*, 1.

(4) Wachs, I. E.; Jehng, J. M.; Deo, G.; Weckhuysen, B. M.; Guliants, V. V.; Benziger, J. B. *Catal. Today* **1996**, *32*, 47.

(5) Olthof, B.; Khodakov, A.; Bell, A. T.; Iglesia, E. *J. Phys. Chem. B* **2000**, *104*, 1516.

(6) Wachs, I. E. *Catal. Today* **2005**, *100*, 79.

(7) Burcham, L. J.; Deo, G. T.; Gao, X. T.; Wachs, I. E. *Top. Catal.* **2000**, *11*, 85.

(8) Kondratenko, E. V.; Cherian, M.; Baerns, M.; Su, D. S.; Schlogl, R.; Wang, X.; Wachs, I. E. *J. Catal.* **2005**, *234*, 131.

(9) Magg, N.; Immaraporn, B.; Giorgi, J. B.; Schroeder, T.; Baumer, M.; Dobler, J.; Wu, Z. L.; Kondratenko, E.; Cherian, M.; Baerns, M.; Stair, P. C.; Sauer, J.; Freund, H. J. *J. Catal.* **2004**, *226*, 88.

(10) Keller, D. E.; de Groot, F. M. F.; Koningsberger, D. C.; Weekhuysen, B. M. *J. Phys. Chem. B* **2005**, *109*, 10223.

(11) van Lingen, J. N. J.; Gijzernan, O. L. J.; Weckhuysen, B. M.; van Lenthe, J. H. *J. Catal.* **2006**, *239*, 34.

(12) Baumer, M.; Freund, H. J. *Prog. Surf. Sci.* **1999**, *61*, 127.

(13) Campbell, C. T. *Surf. Sci. Rep.* **1997**, *27*, 1.

(14) Kishi, K.; Hirai, K.; Yamamoto, T. *Surf. Sci.* **1993**, *290*, 309.

(15) Dupuis, A. C.; Abu Haija, M.; Richter, B.; Kuhlenbeck, H.; Freund, H. J. *Surf. Sci.* **2003**, *539*, 99.

(16) Niehus, H.; Blum, R. P.; Ahlbehrendt, D. *Surf. Rev. Lett.* **2003**, *10*, 353.

(17) Surnev, S.; Vitali, L.; Ramsey, M. G.; Netzer, F. P.; Kresse, G.; Hafner, J. *Phys. Rev. B* **2000**, *61*, 13945.

(18) Sambi, M.; Della Negra, M.; Granozzi, G. *Thin Solid Films* **2001**, *400*, 26.

(19) Magg, N.; Giorgi, J. B.; Schroeder, T.; Baumer, M.; Freund, H. J. *J. Phys. Chem. B* **2002**, *106*, 8756.

(20) Kaya, S.; Weissenrieder, J.; Stacchiola, D.; Shaikhutdinov, S.; Freund, H. J. *J. Phys. Chem. C* **2006**, *111*, 759.

(21) Wendt, S.; Frerichs, M.; Wei, T.; Chen, M. S.; Kempter, V.; Goodman, D. W. *Surf. Sci.* **2004**, *565*, 107.

(22) Yan, X. M.; Ni, J.; Robbins, M.; Park, H. J.; Zhao, W.; White, J. M. *J. Nanopart. Res.* **2002**, *4*, 525.

(23) Liang, G.; Perry, S. S. *Surf. Sci.* **2005**, *594*, 132.

(24) Song, D.; Hrbek, J.; Osgood, R. *Nano Lett.* **2005**, *5*, 1327.

(25) Schroeder, T.; Adelt, M.; Richter, B.; Naschitzki, M.; Baumer, M.; Freund, H. J. *Surf. Rev. Lett.* **2000**, *7*, 7.

(26) Weissenrieder, J.; Kaya, S.; Lu, J. L.; Gao, H. J.; Shaikhutdinov, S.; Freund, H. J.; Sierka, M.; Todorova, T. K.; Sauer, J. *Phys. Rev. Lett.* **2005**, *95*, 076103.

(27) Doniach, S.; Sunjic, M. *J. Phys. C* **1970**, *3*, 285.

(28) Shirley, D. A. *Phys. Rev. B* **1972**, *5*, 4709.

(29) Todorova, T. K.; Sierka, M.; Sauer, J.; Kaya, S.; Weissenrieder, J.; Lu, J. L.; Gao, H. J.; Shaikhutdinov, S.; Freund, H. J. *Phys. Rev. B* **2006**, *73*, 165414.

(30) Kuhlenbeck, H.; Freund, H. J. Adsorption of Molecules on Metal, Semiconductor and Oxide Surfaces. In *Landolt-Börnstein: Numerical Data and Functional Relationships in Science and Technology - New Series*; Bonzel, H. P., Ed.; Springer-Verlag: Berlin; Heidelberg; New York, 2006; Vol. 42, p 332.

(31) Sawatzky, G. A.; Post, D. *Phys. Rev. B* **1979**, *20*, 1546.

(32) Giordano, L.; Del Vitto, A.; Pacchioni, G. *J. Chem. Phys.* **2006**, *124*.

(33) Sierka, M.; Todorova, T. K.; Kaya, S.; Stacchiola, D.; Weissenrieder, J.; Lu, J.; Gao, H.; Shaikhutdinov, S.; Freund, H. J.; Sauer, J. *Chem. Phys. Lett.* **2006**, *424*, 115.

(34) Schoiswohl, J.; Sock, M.; Surnev, S.; Ramsey, M. G.; Netzer, F. P.; Kresse, G.; Andersen, J. N. *Surf. Sci.* **2004**, *555*, 101.

(35) Sock, M.; Surnev, S.; Ramsey, M. G.; Netzer, F. P. *Top. Catal.* **2001**, *14*, 15.

(36) Davydov, A. A.; Rochester, C. H. *Infrared spectroscopy of adsorbed species on the surface of transition metal oxides*; Wiley: Chichester, New York, 1990.

(37) Carter, S. A.; Yang, J.; Rosenbaum, T. F.; Spalek, J.; Honig, J. M. *Phys. Rev. B* **1991**, *43*, 607.

(38) Shin, S.; Suga, S.; Taniguchi, M.; Fujisawa, M.; Kanzaki, H.; Fujimori, A.; Daimon, H.; Ueda, Y.; Kosuge, K.; Kachi, S. *Phys. Rev. B* **1990**, *41*, 4993.

(39) Luo, Q.; Guo, Q. L.; Wang, E. G. *Appl. Phys. Lett.* **2004**, *84*, 2337.

(40) Toledano, D. S.; Metcalf, P.; Henrich, V. E. *Surf. Sci.* **2000**, *449*, 19.

(41) Schuler, H.; Klimm, S.; Weissmann, G.; Renner, C.; Horn, S. *Thin Solid Films* **1997**, *299*, 119.

(42) Demeter, M.; Neumann, M.; Reichelt, W. *Surf. Sci.* **2000**, *454*, 41.

(43) Surnev, S.; Ramsey, M. G.; Netzer, F. P. *Prog. Surf. Sci.* **2003**, *73*, 117.

(44) Abu Haija, M.; Guimond, S.; Uhl, A.; Kuhlenbeck, H.; Freund, H. J. *Surf. Sci.* **2006**, *600*, 1040.

(45) Schoiswohl, J.; Tzvetkov, G.; Pfuner, F.; Ramsey, M. G.; Surnev, S.; Netzer, F. P. *Phys. Chem. Chem. Phys.* **2006**, *8*, 1614.

(46) Wang, L. Q.; Baer, D. R.; Engelhard, M. H.; Shultz, A. N. *Surf. Sci.* **1995**, *344*, 237.

(47) Maurice, V.; Cadot, S.; Marcus, P. *Surf. Sci.* **2001**, *471*, 43.

(48) Henderson, M. A. *Surf. Sci. Rep.* **2002**, *46*, 5.

(49) Uchida, N.; Kittaka, S. *J. Phys. Chem.* **1994**, *98*, 2129.

(50) Concepcion, P.; Reddy, B. M.; Knozinger, H. *Phys. Chem. Chem. Phys.* **1999**, *1*, 3031.

(51) Wang, C. B.; Deo, G.; Wachs, I. E. *J. Catal.* **1998**, *178*, 640.

(52) Busca, G.; Ramis, G.; Lorenzelli, V. *J. Mol. Catal.* **1989**, *50*, 231.

(53) Boccuzzi, F.; Coluccia, S.; Ghiotti, G.; Morterra, C.; Zecchina, A. *J. Phys. Chem.* **1978**, *82*, 1298.

(54) Morrow, B. A.; McFarlan, A. J. *J. Phys. Chem.* **1992**, *96*, 1395.

(55) Chakarov, D.; Kasemo, B. *Phys. Rev. Lett.* **1998**, *81*, 5181.

(56) Petrik, N. G.; Kimmel, G. A. *Phys. Rev. Lett.* **2003**, *90*.

(57) Smith, R. S.; Kay, B. D. *Nature* **1999**, *398*, 788.

(58) McClure, S. M.; Safarik, D. J.; Truskett, T. M.; Mullins, C. B. *J. Phys. Chem. B* **2006**, *110*, 11033.

(59) Henderson, M. A. *Langmuir* **1996**, *12*, 5093.

(60) Leist, U.; Ranke, W.; Al-Shamery, K. *Phys. Chem. Chem. Phys.* **2003**, *5*, 2435.

(61) Surnev, S.; Sock, M.; Kresse, G.; Andersen, J. N.; Ramsey, M. G.; Netzer, F. P. *J. Phys. Chem. B* **2003**, *107*, 4777.

(62) Magg, N.; Giorgi, J. B.; Hammoudeh, A.; Schroeder, T.; Baumer, M.; Freund, H. J. *J. Phys. Chem. B* **2003**, *107*, 9003.